Cytotoxic and genotoxic assessment of glycolipid-reduced and -capped gold and silver nanoparticles†

Sanjay Singh,‡[a] V. D'Britto,[a] A. A. Prabhune,[b] C. V. Ramana,[a] Alok Dhawan*[c] and B. L. V. Prasad*[a]

Received (in Victoria, Australia) 22nd June 2009, Accepted 29th September 2009
First published as an Advance Article on the web 24th November 2009
DOI: 10.1039/b9nj00277d

A systematic cytotoxic and genotoxic evaluation of glycolipid-conjugated silver and gold nanoparticles is carried out. These glycolipid nanoparticle conjugates are obtained by exploiting the reductive capability of a class of glycolipids called sophorolipids that play the role of capping agent as well. Further, when tested for their cytotoxicity and genotoxicity on HepG2 cells, these nanoparticles are found to be cytocompatible up to 100 μM metal concentrations. Of the two metallic systems investigated, gold nanoparticles are found to be more cytocompatible than the same concentrations of silver nanoparticles. Similarly, it is also demonstrated that at 100 μM, silver nanoparticles cause more DNA damage compared to gold nanoparticles of similar concentrations.

Introduction

One of the reasons nanoscience and technology have crossed the researchers' domain and aroused the interest of common people is their perceived biomedical applications.[1] Even in the broad arena of biomedical applications, metal nanoparticles have caught the attention of researchers and common people alike as drug delivery agents,[2] diagnostic tools[3] and even as therapeutics.[4] In this background, the view of toxicological evaluation of nanomaterials is being shifted from an "accidental entry" possibility to a "deliberate placment" likelihood in the human body.[5] Many groups have studied the uptake of these nanoparticles into various cell types. Amongst these, silver nanoparticles (AgNPs) and gold nanoparticles (AuNPs) constitute the main classes of nanoparticle systems studied. A report by Shukla *et al.*[6] suggests that AuNPs are non-cytotoxic to macrophages, which is attributed to the reduced production of reactive oxygen species and nitrite species. A cytotoxicity study conducted by Connor *et al.*[7] shows that AuNPs are taken up by human leukemia cells but are not necessarily toxic to cellular functions. Cytotoxicity evaluations of AgNPs carried out on L929 fibroblasts by Yu *et al.*,[8] suggest that these nanoparticles are biocompatible at lower concentrations only. On the other hand, Hussain *et al.*[9] report that AgNPs are highly toxic to BRL3A rat liver cells and Valiyaveettil's group has also shown AgNPs to be highly toxic to human lung fibroblast cells (IMR-90) and human glioblastoma (U251) cells.[10] The studies mentioned above indicate that the uptake and response of cells towards nanoparticles are mainly dependent on two factors: first, the method of synthesis and composition of the nanoparticle and, second, the cell type used. In this context, glycolipid-conjugated metal nanoparticles have recently been pursued with great vigor for their potential bio-applications.[11] We have been looking at sophorolipids that are available through bio-mediated processes as a means to achieve glycolipid–nanoparticle conjugates in one step as these sophorolipids are capable of reducing metal ions like Au^{3+} and Ag^{+}, and thereafter capping the ensuing metal nanoparticles. We have already shown that sophorolipid reduced/capped silver nanoparticles are good bactericidal agents.[12] While we are also investigating their potential as drug delivery agents, one of the important questions that may arise is their cytotoxicity and, at a more intricate level, their genotoxicity, as many of the nanoparticle-based drug delivery agents are targeted at the cell nucleus.[13] Keeping this fact in mind, we embarked on an investigation of the cytotoxic and genotoxic effects of sophorolipid reduced/capped silver and gold nanoparticles. Moreover, the fate of the ingested particles leads them to accumulate in certain organs of the body, the liver being one of them. Therefore, we have chosen a hepatic cell line in order to investigate the cytotoxic effects of glycolipid-synthesized AuNPs and AgNPs. HepG2 cells (human hepatocellular cell line) were exposed to different concentrations of metal nanoparticle suspensions and their responses are presented below in detail.

Materials and methods

Materials

Chloroauric acid ($HAuCl_4$) was purchased from SRL chemicals and used as received. Ethyl methanesulfonate (EMS; CAS No. 62-50-0), normal melting point agarose (NMA), low melting

[a] *Materials Chemistry Division, National Chemical Laboratory, Pune-411 008, India. E-mail: pl.bhagavatula@ncl.res.in; Fax: +91 20 25902636; Tel: +91 20 25902013*
[b] *Division of Biochemical Sciences, National Chemical Laboratory, Pune-411008, India*
[c] *Nanomaterial Toxicology Group, Indian Institute of Toxicology Research, Lucknow-226001, India. E-mail: alokdhawan@iitr.res.in*

† Electronic supplementary information (ESI) available: Additional UV-vis and FTIR spectra, transmission electron, phase contrast and optical microscope images and statistical data. See DOI: 10.1039/b9nj00277d

‡ Current address: Department of Molecular Biology and Microbiology, Burnett School of Biomedical Sciences, College of Medicine, University of Central Florida, Orlando, FL 32816, USA.

point agarose (LMPA), and ethidium bromide (EtBr) were purchased from Sigma Chemicals (St. Louis, MO). Ca^{2+} and Mg^{2+} ion-free phosphate buffer saline (PBS), malt extract, glucose, yeast extract, peptone MTT (3-(4,5-dimethylthiazoyl-2-yl)-2,5-diphenyltetrazolium bromide), Triton X-100 and disodium EDTA were purchased from Hi-Media (Mumbai, India). DMSO was procured from Qualigens, India and Trizma Base was purchased from Spectrochem. All other chemicals were obtained locally and were of analytical reagent grade. EMS, a well-known mutagen,[14] was used as a positive control in this study.

Synthesis of sophorolipid (OA-SL), OA-SL-reduced gold nanoparticles (OA-SL-AuNPs) and OA-SL-reduced silver nanoparticles (OA-SL-AgNPs)

The sophorolipid (OA-SL) was synthesized from oleic acid (OA) through its transformation by a yeast species (*Candida bombicola*) in 10% glucose medium. The details of synthesis, purification and characterization of OA-SL molecules have been described in our previous reports.[12,15] For the synthesis of OA-SL-AuNPs, OA-SL (1×10^{-4} M) was added to an aqueous solution of $HAuCl_4$ (1×10^{-4} M) and this mixture was incubated for 12 h. The development of a purple color indicated the formation of AuNPs which was further confirmed by UV-visible spectroscopy and TEM measurements *etc*. Dialyzing for 24 h with a dialysis membrane having a 12 kDa molecular weight cut-off, leads to purification of this AuNP suspension. This purified suspension was centrifuged and the pellet was air dried. The ensuing powder was used for further characterizations. OA-SL-AgNPs were synthesized and purified by the method described in our previous report.[12]

To test the changes in the surface characteristics of OA-SL-capped nanoparticles when they are incubated with different media and buffer, the powders of these nanoparticles, obtained after centrifuging and drying, were incubated with the respective media and buffer. Aliquots from the solutions were drawn at different time intervals and these were subjected to UV-vis, Fourier transform infra red (FTIR) and transmission electron microscopy (TEM) analyses.

Sample characterizations

Samples for TEM were prepared by drop-coating the isolated and resuspended solution on carbon-coated copper grids. TEM measurements were performed on a JEOL model 1200EX instrument operated at an accelerating voltage of 120 kV. X-Ray diffraction (XRD) measurements of drop-coated films of reaction products on a glass substrate were carried out on a PANalytical Xpert Pro instrument operated at a voltage of 40 kV and a current of 30 mA with Cu Kα radiation. UV-vis spectra of OA-SL-AuNPs were monitored on a Jasco-V-570 UV-vis/NIR spectrophotometer operated at a resolution of 2 nm. Thermogravimetric analysis (TGA) was done on a TA Instruments model no Q 600, ambient to 900 °C. Samples were run at 10 mL min^{-1} N_2 flow and at 10 °C min^{-1} heating rate, using the dried powder of OA-SL-AuNPs and OA-SL-AgNPs. The amount of OA-SL for a given weight of sample was calculated on the basis of % weight loss.

Cell lines

HepG2 cell line (human hepatocellular cell line) was used for cytotoxicity and genotoxicity studies of OA-SL-AuNPs and OA-SL-AgNPs. The HepG2 cells (ATCC No. HB-8065), initially procured from the National Center for Cell Science, Pune, India have been maintained further at the Indian Institute of Toxicology Research, Lucknow, India. The cells were maintained in minimum essential medium (MEM) supplemented with 10% fetal bovine serum (FBS), 1 mM sodium pyruvate, 2 mM glutamine, 50 U mL^{-1} penicillin, 50 mg mL^{-1} streptomycin and 100 mM non-essential amino acids. Cells were cultured for 3–4 d (~80% confluency) before the assay.

Sample preparation for MTT assay

Solutions of OA-SL-AuNPs and OA-SL-AgNPs were centrifuged separately to give a pellet. The pellets were weighed and resuspended in 1 mL of Milli-Q water to make stock solutions from which the working nanoparticle suspension was prepared by the serial dilution method. The weights of metal and OA-SL present in each case were evaluated by TGA. The metal weight was also independently determined by AAS. The results from AAS and TGA were in accordance with each other within experimental error. Thus, at the highest concentration, the total weight of OA-SL-AuNPs used was 51.4 μg mL^{-1} while that of OA-SL-AgNPs was 12.75 μg mL^{-1}. These weights were selected to provide a metal concentration close to 100 μM in each case.

MTT assay

The MTT assay was performed following the method described by Mosmann[16] with slight modification. In brief, cells (10 000–15 000 cells/well in 100 μL of medium) were seeded in a 96 well plate and allowed to adhere for 24 h at 37 °C in a 5% CO_2 95% air atmosphere. The medium was replaced with serum-free medium (IMEM) containing different concentrations of OA-SL-AuNPs or OA-SL-AgNPs and incubated for 3 h at 37 °C. The treatments were discarded and 100 μL serum-free medium and 10 μL MTT (5 mg mL^{-1}) in PBS were added to each well and re-incubated for another 4 h at 37 °C. The reaction mixture was carefully discarded and 200 μL of DMSO was added to each well and mixed thoroughly. After 10 min, the absorbance was read at 530 nm, using a multiwell microplate reader (Biotek, USA). The untreated sets were also run in parallel under identical conditions and served as the control. The relative cell viability in percentage could be calculated as:

$$(A530 \text{ of treated samples}/A530 \text{ of untreated samples}) \times 100$$

where, $A530$ is the absorbance at 530 nm. The data presented are the means ± standard deviation (SD) from three independent experiments.

Morphological analysis

The morphologies of cells before and after the OA-SL-AuNPs or OA-SL-AgNPs treatments were examined under a phase-contrast inverted microscope (Leica Germany). The changes in the cells were quantified using automatic image analysis

software Leica Q Win 500, connected with the inverted phase-contrast microscope.

Comet assay

In a typical experiment, cells (70 000–80 000 cells/well in 1 mL of medium) were seeded into two separate 12-well plates and allowed to adhere for 24 h at 37 °C in an atmosphere of 5% CO_2 95% air. In both the plates, the medium was replaced with serum-free medium containing OA-SL-AuNPs or OA-SL-AgNPs of different concentrations and incubated for 3 h at 37 °C. After incubation, the medium was replaced with PBS and washed thoroughly. Cells were then gently harvested with 0.4 mL of 0.025% trypsin (in PBS). The effect of trypsin was nullified by adding 0.3 mL of CMEM (supplemented with 10% FBS) and collected in eppendorf tubes. Additionally, wells were rinsed with 0.3 mL of PBS and collected in the same eppendorf tube. The COMET assay was performed according to the method described by Singh *et al.* with slight modification.[17] In brief, cell pellets were obtained by centrifugation (5000 rpm, 5 min), which were again resuspended in 100 μL of PBS. To this, 100 μL of 1% LMPA (low melting point agarose) was added, mixed well at 37 °C and finally 80 μL of cell suspension was layered on top of the end-frosted slides that were pre-coated with 1% normal melting point agarose. Then, cover slips (24 × 60 mm) were placed on top of the slides and were kept at 4 °C. After 5 min, the cover slips were removed and 90 μL of 0.5% LMPA was again layered on top of the slides before replacing the cover slips and keeping the slides at 4 °C again. After overnight lysis at 4 °C in freshly-prepared lysing solution (2.5 M of NaCl, 100 mM of EDTA, 10 mM of Tris, and 1% Triton X-100, pH 10), slides were kept in an electrophoretic unit (Life Technologies, Gaithersburg, MD), filled with chilled and freshly prepared electrophoresis buffer (1 mM Na_2EDTA and 300 mM NaOH, pH ~ 13). The slides were left (in the electrophoresis solution) for 30 min to allow unwinding of DNA. Following the unwinding, electrophoresis was performed for 30 min at 0.7 V cm^{-1} using a power supply from Techno Source (Mumbai, INDIA). To prevent DNA damage from stray light, if any, all the steps starting from single cell preparation were performed under dimmed light. After electrophoresis, the slides were immediately neutralized with 0.4 M of Tris buffer (pH 7.5) for 5 min and the neutralizing process was repeated three times for 5 min each. The slides were then stained with ethidium bromide (20 μg mL^{-1}: 75 μL per slide) for 10 min in the dark. After staining, the slides were dipped once in chilled distilled water to remove the excess stain and, subsequently, fresh cover slips were placed over them.

The slides were examined after 2 h of staining, using an image analysis system (Kinetic Imaging, Liverpool, UK) attached to a fluorescent microscope (Leica, Germany). The images were transferred to a computer through a charge-coupled device camera and analyzed using Komet 5.0 software. All the experiments were conducted in triplicate and the slides were prepared in duplicate. Twenty five cells per slide, equalling 150 cells per group, were randomly captured at a constant gel depth, avoiding the cells present at the edges and superimposed comets.

Data analysis

Data are presented as the means ± SD. Statistical analysis was carried out by analysis of variance (ANOVA). The level of statistical significance was set at $P < 0.05$ and $P < 0.01$ wherever required and labeled by an asterisk (*).

Results and discussions

The OA-SL-mediated synthesis of OA-SL-AuNPs and OA-SL-AgNPs by reduction of Au^{+3} and Ag^{+} ions was confirmed by UV-visible, TEM and XRD spectra *etc.* Fig. 1A (curve 1—AgNPs and curve 2—AuNPs) represents the typical UV-visible spectra characteristic of the respective nanoparticle systems.[18] XRD patterns (Fig. 1B; trace A—AgNPs and trace A—AuNPs), recorded from the films formed by drop-casting of aqueous suspensions on a glass substrate, show the characteristic Bragg reflections, indexed for the [111], [200], [220] and [311] planes, of crystalline silver (trace A) and gold (trace B).[19] The presence of broadened XRD signals again suggests a small particle size. TEM images (Fig. 1C—AgNPs and Fig. 1D—AuNPs) reveal the formation of nanoparticles having ~15–20 nm (AgNPs) and ~10 nm (AuNPs) diameters. Clusters of OA-SL-AuNPs can be seen in Fig. 1D which could be assigned to the interaction between OA-SL molecules, as the self assembly of glycolipid molecules in water at ambient conditions is well known.[20] The aggregated structures seen under TEM are most probably due to the solvent evaporation effect as the sharp peak at 520 nm in the UV-vis spectrum unambiguously indicates that the nanoparticles are well separated from each other.

These results indicate that OA-SL molecules can efficiently reduce gold and silver ions into their respective nanoparticles at ambient conditions. The amount of OA-SL molecules present along with AuNPs and AgNPs was calculated by TGA (Fig. 2A and B). The figure clearly indicates that the weight loss takes place in two major regions in the case

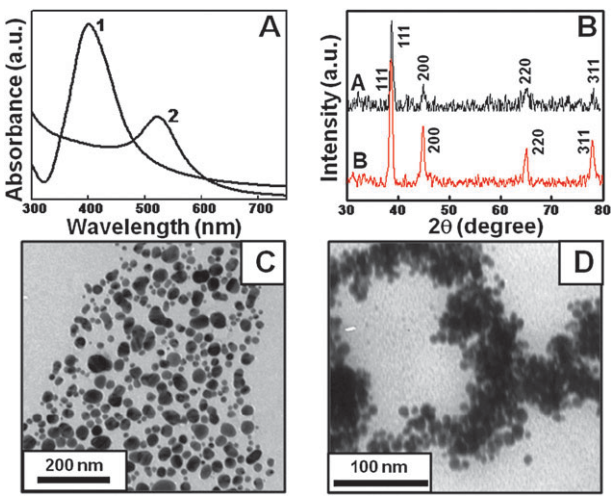

Fig. 1 OA-SL-mediated synthesis of AuNPs and AgNPs. (A) UV-visible spectra recorded from OA-SL-AgNPs (trace 1) and OA-SL-AuNPs (trace 2); (B) XRD patterns obtained from OA-SL-AgNPs (trace A) and OA-SL-AuNPs (trace B); TEM images taken from OA-SL-AgNPs (C) and OA-SL-AuNPs (D).

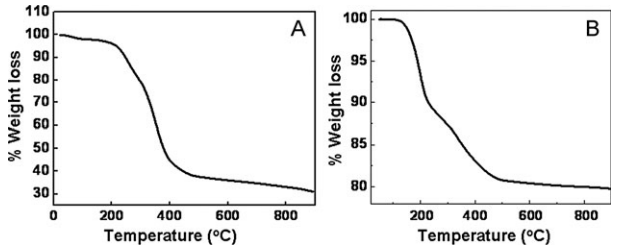

Fig. 2 TGA analysis performed on dried powder of OA-SL-AuNPs (A) and OA-SL-AgNPs (B) showing two major regions of weight loss.

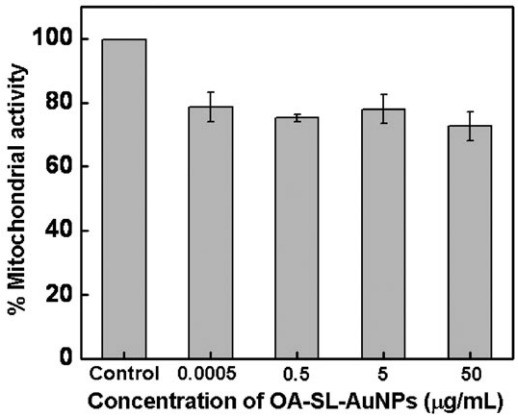

Fig. 3 Cell viability (MTT) assay of HepG2 cells incubated with different concentrations of OA-SL-AuNPs for 3 h.

of OA-SL-AuNPs. The first region appears around 200 °C (~30% weight loss) and the second region being around 330 °C (~40% weight loss) thus corresponding to total weight loss of 70%. In case of OA-SL-AgNPs, the weight loss also occurs in two regions, the first at 200 °C (~10% weight loss), and the second at around 300 °C (~10% weight loss), giving a total weight loss of 20%.

These metal nanoparticles were further tested for their toxicity on HepG2 (human hepatocellular cell line: ATCC No. HB-8065) cell lines. The toxicity study included a cell viability test (MTT assay) and genotoxicity test (COMET assay). The cytotoxicity assessment involves the use of MTT dye, which is converted into formazan crystals by the mitochondrial succinate dehydrogenase enzyme. This conversion is a direct evidence of the viability of cells. Further, the comet assay, or single cell gel electrophoresis, is a sensitive and powerful technique for the detection of DNA at the eukaryotic cell level. It has gained popularity as a tool for detection of DNA damage/repair, bio-monitoring and genotoxicity testing. It is based upon three parameters, which include tail length (TL, μm), tail DNA (TDNA, %) and Olive tail moment (OTM, arbitrary units). OTM is the distance between the centre of mass of the tail and the centre of mass of the head, in micrometers, multiplied by the percentage of DNA in the tail. The comet assay is considered to be an accurate and sensitive parameter, as it takes into account both the quality and quantity of DNA damage.

It is well known that nanomaterials show different physicochemical properties when dispersed in different solvents,[21] which might affect their toxicological properties as well. We, therefore, characterized the OA-SL-AuNPs and OA-SL-AgNPs dispersed in common biological dispersion media such as PBS and serum (10% FBS) containing cell culture media (CMEM). Here, the UV-vis spectra and the TEM images reveal discernable changes in the surface plasmon peak positions compared to the dispersed samples in water (ESI-1, ESI-2†) and indicate the presence of significant aggregation and the presence of a 'bright' material surrounding these clusters in the TEM images. The FTIR spectra recorded from OA-SL-AuNPs dispersed in PBS buffer (ESI-3†, trace 3) and CMEM (ESI-3†, trace 4) point to significant changes in the spectral patterns indicating the possibility of changes occurring on the nanoparticle surface due to exchanges between the capping SL molecules and the different molecules present in these media. OA-SL-AgNPs dispersed in PBS buffer (ESI-4†, trace 3) also reveal similar trends. Thus, all the above analysis point to the exchanges of SL molecules with the molecules present in the media/buffer. These results are consistent with earlier results, where the formation of a "protein corona" over a NP surface when exposed to protein-containing dispersion medium has been reported.[22] Interestingly, in both OA-SL-AuNPs and OA-SL-AgNPs cases there is very little change in the UV-vis absorbance spectra before and after incubation with serum-free media. Therefore, we performed the cytotoxicity and genotoxicity experiments in serum-free media (IMEM).

In the following discussion, we describe, in detail, the cytotoxic and genotoxic effects of OA-SL-AuNPs and OA-SL-AgNPs and pure SL molecules. Fig. 3 represents the MTT assay results due to the interaction of HepG2 cells with OA-SL-AuNPs at different concentrations. It shows that lower concentrations of OA-SL-AuNPs (0.0005, 0.51 and 5.14 μg mL^{-1}) were not toxic to cells. A cell viability of ~78% was recorded, against 100% in the case of untreated cells serving as the control. These results were again supported by phase contrast microscopic images (ESI-5†), recorded from the cells treated with the above mentioned concentrations of OA-SL-AuNPs. Healthy cells were marked with extended cell morphology and seen to be adhered to the plate surface, even after treatment with the concentrations of OA-SL-AuNPs mentioned above, much resembling the untreated cells (control cells shown in ESI-5A†). It is observed that when these cells were treated with a higher concentration, 51.4 μg mL^{-1}, of OA-SL-AuNPs, the cell viability decreased further to ~72% suggesting a slight, yet negligible, toxic effect of nanoparticles. This was further supported by the change in cell morphology from elongated (ESI-5A†) to a roughly rounded shape (ESI-5C†). Further, cell viability was tested against 514 μg mL^{-1} of OA-SL-AuNPs (MTT data not shown) which resulted in complete suppression of cell viability as no viable cell image was recorded (ESI-5B†), only cell debris could be seen. The black spots could be assigned to the presence of OA-SL-AuNPs. Thus, from the MTT assay results, it can be concluded that OA-SL-AuNPs with a gold content concentration below 51.4 μg mL^{-1} are not toxic.

Further, OA-SL-AuNPs dispersed in PBS and CMEM, exposed to cells for 24, 48 and 72 h, were also tested for cytotoxicity. OA-SL-AuNPs dispersed in PBS (ESI-6†) were found to be non-toxic (>90% cell viability). The cell viability

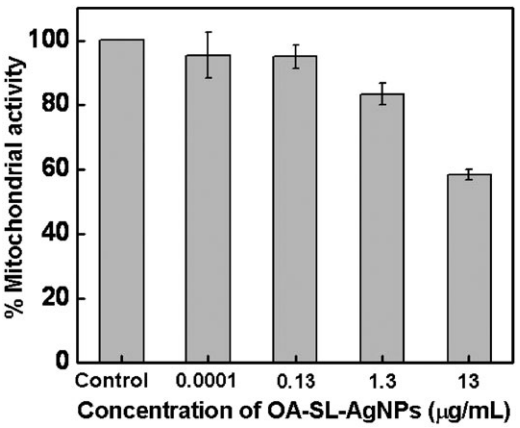

Fig. 4 Cell viability (MTT) assay of HepG2 cells incubated with different concentrations of OA-SL-AgNPs for 3 h.

started showing a downward trend (~80% cell viability) after a 72 h exposure with 51.4 μg mL^{-1} concentration. Cells exposed to OA-SL-AuNPs, dispersed in CMEM (ESI-7†) for 24 h did not show any significant toxicity. However, 48 and 72 h exposures showed relatively less cell viability.

Cytotoxicity assessment of OA-SL-AgNPs was also performed on HepG2 cells Fig. 4. In the case of lower concentrations (0.0001, 0.12 and 1.27 μg mL^{-1}) ~90% cell survival was observed, which can be correlated with the optical images showing intact cell morphology (ESI-8D, E and F†) compared to the control cells (ESI-8A†). HepG2 cells treated with these lower concentrations of OA-SL-AgNPs show morphological characteristics almost similar to untreated cells. Further, an exposure of 12.75 μg mL^{-1} OA-SL-AgNPs shows ~58% cell survival which was further corroborated by the corresponding phase contrast micrograph (ESI-8C†). No cells with regular morphology could be seen here. Instead, black aggregates (OA-SL-AgNPs) and damaged cell remains were quite visible. Similar to OA-SL-AuNPs, concentrations above 12.75 μg mL^{-1} were not considered for the experiments because at these concentrations OA-SL-AgNPs show formation of aggregates which settle over the cell surface and ultimately lead to cell death (ESI-8B†). Dispersions of OA-SL-AgNPs in PBS (ESI-9†) and CMEM (ESI-10†) were also tested for cytotoxicity against cells for 24, 48 and 72 h. In the case of PBS, an appreciable decrease in cell viability was observed only at higher concentrations, whereas in case of CMEM, the particles do not behave any differently from those dispersed in plain media. At this point, it becomes necessary to mention that the toxic effects of Ag^+ ions are well reported. Hence, cytotoxicity of Ag^+ ions was also tested, which showed tremendous toxicity at higher concentrations, irrespective of dispersion medium (ESI-11†). The MTT assay was based on the reduction of MTT, a tetrazolium dye, by dehydrogenase enzymes. In order to check any ambiguous reaction of MTT dye with the nanoparticles thus leading to the observation reported here, we performed a control experiment with the same experimental settings in the absence of cells. No reduction of MTT dye by the nanoparticles alone (ESI-12 and 13†) can be seen, clearly indicating that the results obtained are due to cellular activities only.

The toxicity studies of OA-SL-AuNPs and OA-SL-AgNPs were further elaborated by performing comet assay which shows the effect of nanoparticles over genetic material (DNA). Fig. 5 shows the change in % tail DNA (Fig. 5A) and olive tail moment (Fig. 5B) with respect to different concentrations of OA-SL-AuNPs. Although MTT assay results show that nanoparticles below 51.4 μg mL^{-1} concentration do not show any significant toxicity, it becomes important that we study the genotoxic effects of the same concentrations. Cytotoxicity assessment is a way to record the response of cells coming into contact with a foreign material, whereas genotoxicity reveals the response of genetic material when cells are exposed to nanoparticles. Thus, it is important that we investigate the genotoxicity of those concentrations that do not actually show any cytotoxicity. Fig. 5A shows % tail DNA pattern of HepG2 cells treated with different concentrations of OA-SL-AuNPs. The lower concentrations (5.14, 0.51 and 0.0005 μg mL^{-1}) show almost similar increases in the % tail DNA pattern (6.29, 6.12 and 6.72 unit) compared to the control (6.08 unit). Further, the comet patterns from the HepG2 cells obtained at these concentrations show intact heads and the complete absence of DNA fragments in the form of a tail (Fig. 5a–e), suggesting that these doses do not cause any DNA damage. However, OA-SL-AuNPs at 51.4 μg mL^{-1} concentration show an increase in % tail DNA (9.02 unit) when compared with the control (6.08 unit). However, this increase in % tail DNA pattern was found to be non-significant when analyzed with ANOVA. From the comet pattern of cell DNA (Fig. 5c), it was again clear that 51.4 μg mL^{-1} concentration of OA-SL-AuNPs shows very little DNA damage and most of the cell DNA was intact in the form of the comet head and looks similar to the control (Fig. 5a). Fig. 5f represents the comet pattern obtained after treatment of cells with EMS, used as a positive control.

Similarly, another comet parameter, OTM (Fig. 5B), was also studied from the DNA of HepG2 cells after treatment with different concentrations of OA-SL-AuNPs (0, 0.0005, 0.51, 5.1 and 51.4 μg mL^{-1}) for 3 h. All concentrations below 51.4 μg mL^{-1} do not show any significant increase in OTM (0.87, 0.86 and 0.89 unit) compared to he control cell OTM (0.87 unit). However, the OTM pattern from the DNA of HepG2 cells treated with 51.4 μg mL^{-1} of OA-SL-AuNPs shows an increase in OTM (1.28 unit) compared to the control (0.87 unit). From the ANOVA analysis, this increase in OTM was not found to be significant, which is in accordance with the results of our MTT assay. This suggests that even though slight DNA damage occurs at this concentration, it was very minute and cannot be considered as toxic.

As per comet assay guidelines[23] and based on our MTT observations, concentrations of OA-SL-AuNPs above 51.4 μg mL^{-1} were not used for the experiments. Also, nanoparticle suspensions of 514 μg mL^{-1} or above were unstable as aggregation was seen which settled at the bottom of the vessel. Further, studying the genotoxicity may not be necessary if the cells show well-defined cytotoxicity.

The effect of OA-SL-AgNPs on DNA of HepG2 cells was determined by a comet assay, performed in a similar way as was done for OA-SL-AuNPs. Fig. 6A shows the % tail DNA pattern of HepG2 cells after 3 h of incubation with different

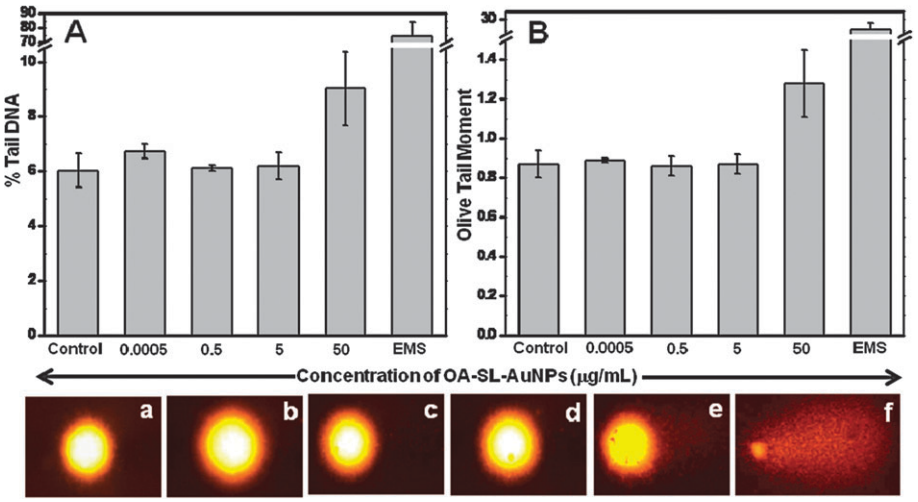

Fig. 5 Comet assay results obtained from exposure of 0.0005, 0.5, 5 and 50 μg mL^{-1} concentrations of OA-SL-AuNPs, and ethyl methanesulfonate (EMS; positive control), to HepG2 cells. Two comet parameters, % tail DNA (A) and olive tail moment (arbitrary units) (B), were taken into account to measure DNA damage. Panels b, c, d and e show the comet pattern obtained after the incubation of 0.0005, 0.5, 5 and 50 μg mL^{-1} of OA-SL-AuNPs with HepG2 cells, respectively. Panel a shows the comet pattern recorded from the untreated HepG2 cells. Panel f is the comet pattern obtained after treatment of cells with EMS (magnification ×400).

concentrations of OA-SL-AgNPs (0.0001, 0.12, 1.27 and 12.75 μg mL^{-1}). The lower concentrations of OA-SL-AgNPs (0.0001, 0.12 and 1.27 μg mL^{-1}) show a similar extent of % tail DNA (6.25, 6.05 and 7.49 unit) as the untreated cells (6.26 unit), suggesting the non-genotoxic effect of OA-SL-AgNPs at these concentrations. These observations were again supported by the comet pattern of respective OA-SL-AgNPs concentrations (Fig. 6a–e). However, OA-SL-AgNPs at 12.75 μg mL^{-1} concentration cause an increase in % tail DNA (9.52 unit) compared to untreated cells (6.26 unit). This increase in % tail DNA was found to be non-significant when analyzed with ANOVA, suggesting that although 12.75 μg mL^{-1} concentration of OA-SL-AgNPs causes a little DNA damage, this dose cannot be considered as genotoxic. These results can again be correlated with MTT assay results, obtained after 3 h incubation of HepG2 cells with OA-SL-AgNPs (12.75 μg mL^{-1}). The comet pattern of HepG2 cells treated with a 12.75 μg mL^{-1} concentration of OA-SL-AgNPs (Fig. 6b) also shows an intact DNA head with very little amount of DNA present in the form of a tail. Another comet parameter, OTM, was analyzed after 3 h incubation of HepG2 cells with OA-SL-AgNPs. In this case also, lower concentrations (0.0001, 0.12 and 1.27 μg mL^{-1}) show almost the same amount of OTM (0.89, 0.86 and 1.01 unit) as was recorded for untreated cells (0.83 unit). HepG2 cells treated with 12.75 μg mL^{-1} OA-SL-AgNPs showed an increased OTM value (1.55 unit) compared to untreated cells (0.83 unit), which was again non-significant under ANOVA analysis. These

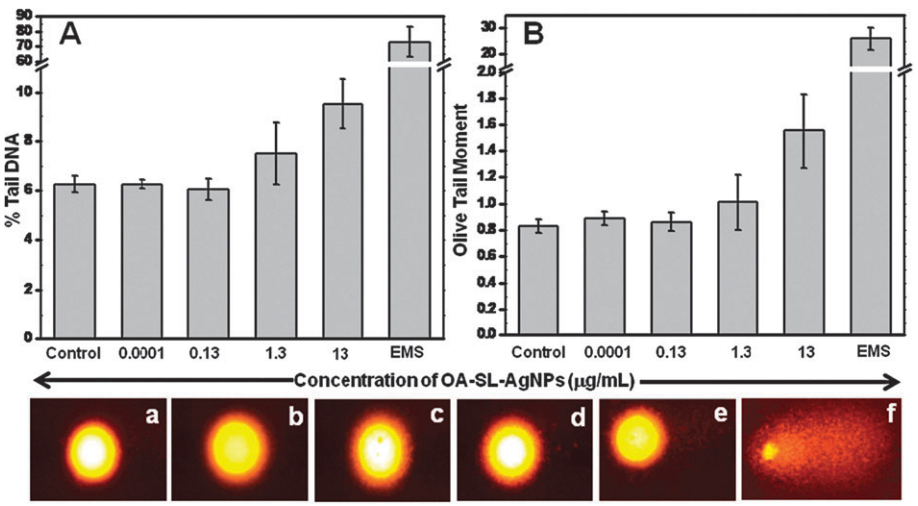

Fig. 6 Comet assay results obtained from the exposure of 0.0001, 0.13, 1.3 and 13 μg mL^{-1} of OA-SL molecules, and ethyl methanesulfonate (EMS; positive control), to HepG2 cells. Two comet parameters, % tail DNA (A) and olive tail moment (arbitrary units) (B), were taken into account to measure DNA damage. Panels b, c, d and e show the comet pattern obtained after the incubation of 0.0001, 0.13, 1.3 and 13 μg mL^{-1} of OA-SL molecules with HepG2 cells respectively. Panel a shows the comet pattern recorded from the untreated HepG2 cells. Panel f is the comet pattern obtained after treatment of cells with EMS (magnification ×400).

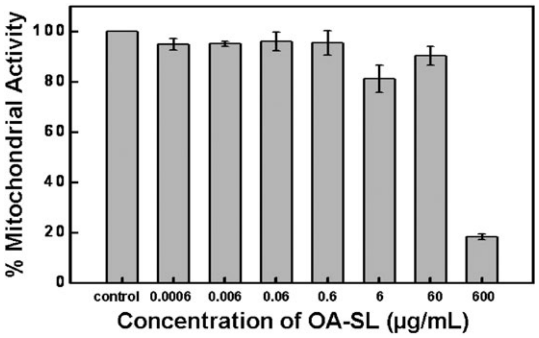

Fig. 7 Cell viability (MTT) assay of HepG2 cells incubated with different concentrations of OA-SL molecules for 3 h.

results were further supported by comet patterns obtained from respective OA-SL-AgNPs-treated HepG2 cells (Fig. 6a–e).

When the cells are treated with OA-SL-AuNP and OA-SL-AgNP systems, it is obvious that the capping agent first comes in contact with the cells. Thus, it becomes imperative to test the cytotoxic and genotoxic effects of pure SL molecules on HepG2 cell lines. Results from previous literature,[24,25] also indicate that it is essential to test the response of cells toward the capping molecule. Therefore, MTT and comet assays for pure OA-SL molecules alone were also conducted, as it is the only capping molecule on OA-SL-AuNPs and OA-SL-AgNPs. From the TGA results, we could easily deduce that about ~40 and ~2.55 μg mL^{-1} of sophorolipid molecules are present on the surfaces of OA-SL-AuNPs and OA-SL-AgNPs, respectively, used in this study. Fig. 7 shows the cytotoxicity response of HepG2 cells to different concentrations of pure SL molecules exposed for 3 h. The lower concentrations (60, 6, 0.6, 0.06, 0.006 and 0.0006 μg mL^{-1}) show ~90% of cell survival, which could again be confirmed by cell morphology images (ESI-14†). Optical images of cells treated with these concentrations of SL molecules show well-adhered and elongated cell morphology. Although some cells of rounded morphology can also be seen, their population was much less and this could be assigned to the normal cell death after completion of their cell cycle, which can be seen in the untreated cell plate too. Also, it is well known that dead cells lose their elongated morphology and become rounded. The HepG2 cell line is an adherent cell line, and thus their first sign of survival would be adhered cells at the bottom of the culture plate.

However, a 600 μg mL^{-1} concentration of OA-SL molecules was cytotoxic as only ~18% of cell survival was recorded. The corresponding cell morphology can be seen in ESI-14B†. The cells lost their normal elongated structure (as untreated cells exhibit these properties) and showed a rounded morphology, indicating dead cells. Also, the number of cells under a given area reduced significantly, indicating the detachment of dead cells from the culture-plate surface. Therefore, it can be concluded that below 60 μg mL^{-1}, OA-SL molecules are non-cytotoxic to HepG2 cells.

To further elucidate the effect of OA-SL molecules on the DNA of HepG2 cells, a comet assay was performed. Fig. 8 shows the extent of DNA damage in HepG2 cells by SL molecules in terms of % tail DNA (Fig. 8A) and OTM (Fig. 8B). Almost no increase in % tail DNA (compared with the control) was recorded when the cells were incubated with different concentrations of OA-SL molecules (60, 6, 0.6 and 0.0006 μg mL^{-1}) for 3 h. Similarly, no increase in OTM was obtained when compared with control (untreated) HepG2 cells (Fig. 8B). These findings were again confirmed from comet pattern images (Fig. 4a–f) obtained from HepG2 cells treated with different concentrations (control, 60, 6, 0.6 and 0.0006 μg mL^{-1}) of OA-SL. This makes it very clear that SL molecules by themselves were not very cytotoxic or genotoxic, especially at 60 μg mL^{-1}. Therefore, the cytotoxic and genotoxic effects observed in OA-SL-AuNPs and OA-SL-AgNPs must be related to the metal system only.

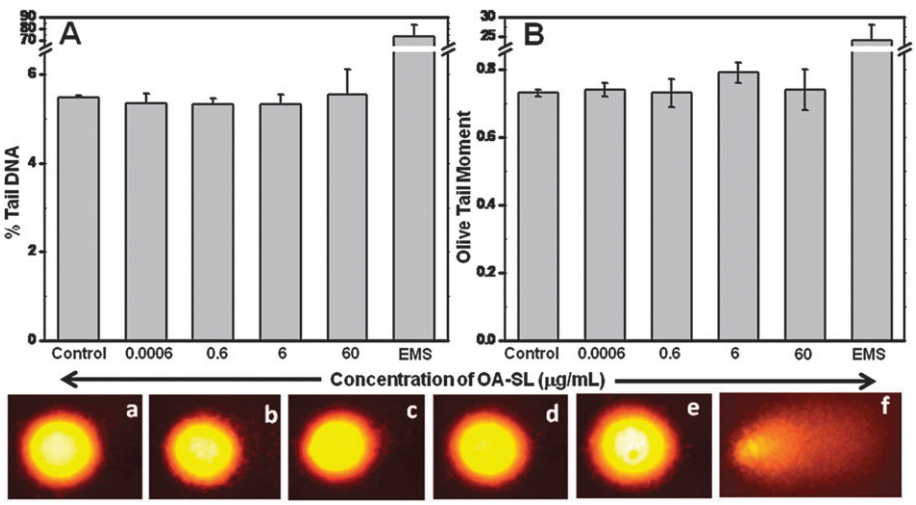

Fig. 8 Comet assay results obtained from the exposure of 0.0006, 0.6, 6 and 60 μg mL^{-1} of OA-SL molecules, and ethyl methanesulfonate (EMS; positive control), to HepG2 cells. Two comet parameters, % tail DNA (A) and olive tail moment (arbitrary units) (B), were taken into account for DNA damage measure. Panels b, c, d and e show the comet pattern obtained after the incubation of 0.0006, 0.6, 6 and 60 μg mL^{-1} of OA-SL molecules with HepG2 cells respectively. Panel a shows the comet pattern recorded from the untreated HepG2 cells. Panel f is the comet pattern obtained after treatment of cells with EMS (magnification ×400).

Interestingly, on comparing the MTT assay data of OA-SL-AuNPs and OA-SL-AgNPs, it was observed that a 12.75 μg mL^{-1} concentration of OA-SL-AgNPs shows only ~58% cell viability while 51.4 μg mL^{-1} OA-SL-AuNPs shows ~72%. It can be easily determined that these concentrations of OA-SL-AuNPs and OA-SL-AgNPs correspond to a metal content of 15.7 μg mL^{-1} (for Au) and 10.20 μg mL^{-1} (for Ag) and to a concentration of ~100 μM in each case. Thus, it can be concluded that between similar concentrations of AgNPs and AuNPs, capped by identical molecules, AgNPs are more toxic (both cyto- and genotoxic). This was in agreement with many earlier results which clearly indicate silver to be more cytotoxic and genotoxic compared to gold. It is well known that AgNPs undergo frequent oxidation compared to AuNPs (Au has a lower reduction potential than Ag). This might lead to the formation of more Ag^+ ions, which are then toxic to the cells; Ag^+ ions have been reported to show more affinity towards "S" (proteins/enzymes) and "P" (DNA/RNA) containing biomolecules, causing their malfunction.[26]

Conclusions

In summary, sophorolipid, a novel glycolipid, is used to synthesize water-dispersible metal nanoparticles at ambient conditions. Further, the prepared OA-SL molecules, AuNPs and AgNPs are tested for their concentration-dependent cytotoxicity and genotoxicity toward human hepatic cells. The nanoparticles are neither cytotoxic nor genotoxic up to concentrations of 100 μM. However, OA-SL-AuNPs show more cytocompatability than OA-SL-AgNPs within a similar concentration range. As the surface chemistry of these sophorolipid-capped particles is very similar to glycolipid-capped ones, the present results may spur more vigorous studies on the other glycolipid-conjugated nanosystems.

Acknowledgements

S.S. and V.B. wish to thank CSIR, New Delhi for Senior Research Fellowship (SRF). B.L.V.P. and A.D. thank the DST for funding under the nanomission programme. A.A.P., C.V.R. and B.L.V.P. also thank DBT for funding.

References

1 (*a*) J. L. West and N. J. Halas, *Annu. Rev. Biomed. Eng*., 2003, **5**, 285–292; (*b*) G. F. Paciotti, L. Myer, D. Weinreich, D. Goia, N. Pavel, R. E. McLaughlin and L. Tamarkin, *Drug Delivery*, 2004, **11**, 169–183; (*c*) K. K. Jain, *Technol. Cancer Res. Treat*., 2005, **4**, 407–416.
2 (*a*) P. Ghosh, G. Han, M. De, C. K. Kim and V. M. Rotello, *Adv. Drug Delivery Rev*., 2008, **60**, 1307–1315; (*b*) G. Han, P. Ghosh, M. De and V. M. Rotello, *NanoBiotechnology*, 2007, **3**, 40–45; (*c*) K. Raghuraman, V. Rahing, C. Cutler, R. Padrapragada, K. K. Katti, V. Kuttumuri, J. D. Robertson, S. J. Casteel, S. Jurisson, C. Smith, E. Boote and K. V. Katti, *J. Am. Chem. Soc*., 2006, **128**, 11342–11343.
3 (*a*) E.-Y. Kim, J. Stanton, B. T. M. Korber, K. Krebs, D. Bogdan, K. Kunstman, S. Wu, J. P. Phair, C. A. Mirkin and S. M. Wolinsky, *Nanomedicine*, 2008, **3**, 293–303; (*b*) N. L. Rosi and C. A. Mirkin, *Chem. Rev*., 2005, **105**, 1547–1562.
4 R. Bhattacharya and P. Mukherjee, *Adv. Drug Delivery Rev*., 2008, **60**, 1289–1306.
5 L. R. Hirsch, R. J. Stafford, J. A. Bankson, S. R. Sershen, B. Rivera, R. E. Price, J. D. Hazle, N. J. Halas and J. L. West, *Proc. Natl. Acad. Sci. U. S. A*., 2003, **100**, 13549–13554.
6 R. Shukla, V. Bansal, M. Chaudhary, A. Basu, R. R. Bhonde and M. Sastry, *Langmuir*, 2005, **21**, 10644–10654.
7 E. E. Connor, J. Mwamuka, A. Gole, C. J. Murphy and M. D. Wyatt, *Small*, 2005, **1**, 325–327.
8 D.-G. Yu, *Colloids Surf., B*, 2007, **59**, 171–178.
9 S. M. Hussain, K. L. Hess, J. M. Gearhart, K. T. Geiss and J. J. Schlager, *Toxicol. in Vitro*, 2005, **19**, 975–983.
10 P. V. AshaRani, G. L. K. Mun, M. P. Hande and S. Valiyaveettil, *ACS Nano*, 2009, **3**, 279–290.
11 (*a*) J. M. De la Fuente and S. Penades, *Biochim. Biophy. Acta*, 2006, **1760**, 636–651; (*b*) J. M. De la Fuente, A. G. Barrientos, T. C. Rojas, J. Rojo, J. Canada, A. Fernandez and S. Penades, *Angew. Chem., Int. Ed*., 2001, **40**, 2257–2261; (*c*) A. G. Barrientos, J. M. De la Fuente, T. C. Rojas, A. Fernandez and S. Penades, *Chem.–Eur. J*., 2003, **9**, 1909–1921; (*d*) C.-C. Lin, Y.-C. Yeh, C.-Y. Yang, G.-F. Chen, Y.-C. Chen, Y.-C. Wu and C.-C. Chen, *Chem. Commun*., 2003, 2920–2921; (*e*) A. C. De Souza, K. M. Halkes, J. D. Meeldijk, A. J. Verkleij, J. F. G. Vliegenthart and J. P. Kamerling, *Eur. J. Org. Chem*., 2004, 4323–4339; (*f*) K. M. Halkes, A. C. De Souza, C. E. P. Maljaars, G. J. Gerwig and J. P. Kamerling, *Eur. J. Org. Chem*., 2005, 3650–3659; (*g*) J. M. de la Fuente, D. Alcántara and S. Penadés, *IEEE Trans. NanoBiosci*., 2007, **6**, 275–281; (*h*) Y. Chen, T. Ji and Z. Rosenzweig, *Nano Lett*., 2003, **3**, 581–584; (*i*) X.-L. Sun, W. Cui, C. Haller and E. L. Chaikof, *ChemBioChem*, 2004, **5**, 1593–1596; (*j*) J. M. de la Fuente and S. Penadés, *Tetrahedron: Asymmetry*, 2005, **16**, 387–391.
12 S. Singh, P. Patel, S. Jaiswal, A. A. Prabhune, C. V. Ramana and B. L. V. Prasad, *New J. Chem*., 2009, **33**, 646–652.
13 S. Dhar, E. M. Reddy, A. Shiras, V. Pokharkar and B. L. V. Prasad, *Chem.–Eur. J*., 2008, **14**, 10244–10250.
14 C. Bilbao, J. A. Ferreiro, M. A. Comendador and L. M. Sierra, *Mutat. Res., Fundam. Mol. Mech. Mutagen*., 2002, **503**, 11–19.
15 M. Kasture, S. Singh, P. Patel, P. A. Joy, A. A. Prabhune, C. V. Ramana and B. L. V. Prasad, *Langmuir*, 2007, **23**, 11409–11412.
16 T. Mosmann, *J. Immunol. Methods*, 1983, **65**, 55–63.
17 N. P. Singh, M. T. McCoy, R. R. Tice and E. L. Schneider, *Exp. Cell Res*., 1988, **175**, 184–191.
18 (*a*) U. Kreibig and M. Volmer, *Optical Properties of Metal Clusters*, Springer Verlag, Berlin, 1996; (*b*) S. Link and M. El-Sayed, *Annu. Rev. Phys. Chem*., 2003, **54**, 331–366; (*c*) P. Mulvaney, *Langmuir*, 1996, **12**, 788–800; (*d*) A. Henglein, *J. Phys. Chem*., 1993, **97**, 5457–5471.
19 XRD spectra were indexed with reference to the crystal structures from the ASTM charts: gold (chart card no. 04-0784) and silver (chart card no. 04-0783).
20 H. Yui, Y. Shimizu, S. Kamiya, I. Yamashita, M. Masuda, K. Ito and T. Shimizu, *Chem. Lett*., 2005, **34**, 232–233.
21 A. Nel, T. Xia, L. Madler and N. Li, *Science*, 2006, **311**, 622–627.
22 A. Nel, L. Mädler, D. Velegol, T. Xia, E. M. V. Hoek, P. Somasundaran, F. Klaessig, V. Castranova and M. Thompson, *Nat. Mater*., 2009, **8**, 543–557.
23 A. Hartmann, E. Agurell, C. Beevers, S. Brendler-Schwaab, B. Burlinson, P. Clay, A. Collins, A. Smith, G. Speit, V. Thybaud and R. R. Tice, *Mutagenesis*, 2003, **18**, 45–51.
24 C. M. Goodman, C. D. McCusker, T. Yilmaz and V. M. Rotello, *Bioconjugate Chem*., 2004, **15**, 897–900.
25 (*a*) T. Niidome, M. Yamagata, Y. Okamoto, Y. Akiyama, H. Takahashi, T. Kawano, Y. Katayama and Y. Niidome, *J. Controlled Release*, 2006, **114**, 343–347; (*b*) H. Takahashi, Y. Niidome, T. Niidome, K. Kaneko, H. Kawasaki and S. Yamada, *Langmuir*, 2006, **22**, 2–5.
26 (*a*) A. Gupta, M. Maynes and S. Silver, *Appl. Environ. Microbiol*., 1998, **64**, 5042–5045; (*b*) Y. Matsumura, K. Yoshikata, S.-I. Kunisaki and T. Tsuchido, *Appl. Environ. Microbiol*., 2003, **69**, 4278–4281.